

Resolving the Scale-Dependence of Mineral Weathering Rates

MARIA E. MALMSTRÖM,^{*,§}
GEORGIA DESTOUNI,[§]
STEVEN A. BANWART,[#] AND
BO H. E. STRÖMBERG[®]

*Department of Civil and Environmental Engineering,
Royal Institute of Technology, AVAT Brinellv. 32,
S-100 44 Stockholm, Sweden, Department of Civil and
Structural Engineering, University of Sheffield,
Mappin Street, Sheffield S1 3JD, United Kingdom, and
Office of Nuclear Waste, Swedish Nuclear Power Inspectorate,
SE-106 58 Stockholm, Sweden*

Comparison between mineral weathering rates determined in the laboratory and in the field commonly reveals large discrepancies, with order(s)-of-magnitude lower rates in the field. Such unresolved scale-dependence seriously limits our ability to extrapolate laboratory results to other scales and conditions. This extrapolation is necessary for quantifying environmental impacts, for instance from acid mine drainage, acid deposition, soil acidification, geological disposal of hazardous waste, and weathering feedback to climate change. We use the well-characterized deposits of mining waste rock at the Aitik site in northern Sweden, for which weathering rates have been previously published, as a model system for investigating this apparent scale-dependence of these rates. We show that the scale-dependence exhibited by the Aitik data is to a large degree predictable by quantification of the effects of a few critical and readily available, bulk-averaged physico-chemical characteristics. The fact that this scale-dependence exhibited by the Aitik data is consistent with other laboratory and watershed studies suggests that at least some of the quantified effects are of general applicability and importance when extrapolating weathering rates from the laboratory to the field.

Introduction

Comparison between mineral weathering rates determined in the laboratory and in the field commonly reveals large discrepancies, with order(s)-of-magnitude lower rates in the field (1–6). Such unresolved scale-dependence seriously limits our ability to extrapolate laboratory results to other scales and conditions. This extrapolation is necessary for quantifying environmental impacts, for instance from acid mine drainage, acid deposition, soil acidification, geological disposal of hazardous waste, and weathering feedback to climate change (7). Inability to generalize and extrapolate laboratory results implies a need for full-scale, costly field investigations at each individual site.

In this study, we make an extended analysis of previously published (8–10) weathering rates for the Aitik waste rock heaps in northern Sweden and attempt to quantitatively account for the observed scale-dependence in the rate data. The previous studies thoroughly assessed sulfide and silicate weathering kinetics over three experimental scales ranging from small batch experiments (10), over large-scale column experiments (9) to field observations (8). In brief, the batch experiments were performed as pH-stat experiments, from which release rates of ions were obtained from the accumulating concentrations of dissolved ions during more than 20 weeks (10). The large-scale columns were operated with free access to the atmosphere and at constant water flow rate. The release rates were obtained at the steady-state conditions observed after 85 weeks of operation (9). In the field, release rates were obtained from the annual average of water flow rates and of concentrations of dissolved ions in two ditches draining the waste rock heaps (8). Table 1 lists characteristics and prevailing conditions for these three scales. The unusually wide range of observation scales, for which data are available for various minerals, makes the Aitik waste rock a potentially useful model system for investigating the apparent scale-dependence of mineral weathering rates. In particular, the existence of large column data (10) represents a rare experimental meso-scale that bridges an important gap between batch experiments and field observations.

The Aitik waste rock heaps in northern Sweden constitute a well-characterized field site (8–12) where the heaps are unsaturated with respect to water and fully oxic over their full depth ((8) oxygen concentrations in the pore gas: 3–21 vol %). The main minerals are quartz, K-feldspar, plagioclase, and mica. Pyrite and chalcopyrite are the dominant sulfides (Table 1 in the Supporting Information). The dominant acidity producing processes are oxidative weathering of pyrite and subsequent oxidation of dissolved ferrous iron (8): $\text{FeS}_{2(s)} + 15/4\text{O}_{2(aq)} + 7/2\text{H}_2\text{O} \rightarrow \text{Fe}(\text{OH})_{3(s)} + 2\text{SO}_4^{2-} + 4\text{H}^+$. The dominant reaction for copper mobilization is oxidative weathering of chalcopyrite (8): $\text{CuFeS}_{2(s)} + 17/4\text{O}_2 + 5/2\text{H}_2\text{O} \rightarrow \text{Cu}^{2+} + 2\text{SO}_4^{2-} + 2\text{H}^+ + \text{Fe}(\text{OH})_{3(s)}$. Available carbonates (mainly calcite) have been depleted to a large degree, leaving the weathering of biotite, $\text{K}(\text{Fe}_{1.5}\text{Mg}_{1.5})(\text{AlSi}_3\text{O}_{10})(\text{OH})_2$, and plagioclase, $(\text{Na}_{0.7}\text{Ca}_{0.3})\text{Al}_{1.3}\text{Si}_{2.7}\text{O}_8$, as the major acidity consuming processes (8). These processes are the main sources of SO_4^{2-} , Cu^{2+} , Mg^{2+} , and Na^+ , which, after release, can be used as tracers for the weathering reactions.

The weathering of silicates and sulfides occurs in successive steps, including reactant/product transport to/from the mineral surface and surface reaction(s). For the Aitik case, the oxic conditions in the heaps (8), the characteristics of the weathered mineral surfaces and the observed temperature dependence of the weathering rates (9) indicate that the weathering processes are controlled by reaction kinetics rather than by diffusion of reactants or products. Microbial mediation of the sulfide weathering is commonly considered to drastically increase the oxidation rate. However, the response of the oxygen consumption rate to a bactericide treatment in the column experiments was relatively low (9), showing that abiotic weathering is important under the prevailing conditions of low temperature and relatively low sulfide content (Table 1).

Using the published (8–10) release rates of SO_4^{2-} , Cu^{2+} , Mg^{2+} , and Na^+ , and the stoichiometry of the weathering reactions, we derived weathering rates (Table 2) for the three

* Corresponding author phone: +46-8-790 87 45; fax: +46-8-790 8689; e-mail: malmstro@ce.kth.se.

§ Royal Institute of Technology.

University of Sheffield.

® Swedish Nuclear Power Inspectorate.

TABLE 1. Characteristics and Prevailing Conditions for the Three Observation Scales, in Terms of Total Waste Rock Mass M , Water Flow Q , Temperature T , pH, and Volumetric Mineral Content γ_m , with the Index M = Pyr, Chalc, Biot, and Plag Denoting the Minerals Pyrite, Chalcopyrite, Biotite, and Plagioclase, Respectively

	M (kg)	Q (m ³ s ⁻¹)	T (°C)	pH	γ_{Pyr} (m ³ m ⁻³)	γ_{Chalc} (m ³ m ⁻³)	γ_{Biot} (m ³ m ⁻³)	γ_{Plag}^a (m ³ m ⁻³)
batch (9)	0.15		20–23	3.3	0.011	0.0025	0.15	0.20
column (10)	1.82×10^3 ^b	9.2×10^{-9}	4–10	≈3.5	0.011	0.0025	0.15	0.20
field (8)	9.5×10^{10} ^b	0.2	1–4	3.8–4.2	0.0057	0.0009	0.080	0.19

^a Plagioclase with a composition corresponding to 70% anorthite and 30% albite. ^b Calculated as $M = HA(1-\epsilon)\rho_s$, where H is height, A is total area, ϵ is porosity, and ρ_s is density of the solid material; in the field (8), the average $H = 20$ m, $A = 2.6 \cdot 10^6$ m², $\epsilon = 0.35$, and $\rho_s = 2.8 \cdot 10^3$ kg m⁻³; in the column experiments (10), $H = 2$ m, $A = 0.5$ m², $\epsilon = 0.35$, and $\rho_s = 2.8 \cdot 10^3$ kg m⁻³.

TABLE 2. Mineral Weathering Rates as Estimated from Observed Tracer Release Rates, in Terms of the Logarithms of the Mass Normalized Weathering Rate R , and the Associated Rate Coefficient $k = R/a_{sm}$, with a_{sm} Being the Specific Surface Area for Mineral m^a

mineral	$\log R^{B,C}$ (mol kg ⁻¹ s ⁻¹)	$\log R^{C,D}$ (mol kg ⁻¹ s ⁻¹)	$\log R^{B,E}$ (mol kg ⁻¹ s ⁻¹)	$\log k^B$ (mol m ⁻² s ⁻¹)	$\log k^C$ (mol m ⁻² s ⁻¹)	$\log k^F$ (mol m ⁻² s ⁻¹)
pyrite	-8.9 ^f	-10.1 ^f	-10.9 ^f	-9.9	-11.1	-11.7
chalcopyrite	-9.5	-11.0	-12.3	-10.0	-11.4	-12.2
biotite	-9.7	-10.6	-11.5	-11.9	-12.8	-13.4
plagioclase	-10.5	-10.9	-11.3	-12.8	-13.2	-13.5

^a The labels B, C, and F refer to the batch, column, and field scale, respectively. ^b Estimated assuming stoichiometric mineral dissolution with Na⁺, Mg²⁺, Cu²⁺, and SO₄²⁻ originating mainly from plagioclase ((Na_{0.7}Ca_{0.3})Al_{1.3}Si_{2.7}O₈), biotite (K(Mg_{1.5}Fe_{1.5})AlSi₃O₁₀(OH)₂), chalcopyrite (CuFeS₂), and pyrite (FeS₂), and chalcopyrite, respectively. ^c Tracer release rate from Strömberg and Banwart ((9) their Table 4, average of triplicates).

^d Tracer release rate from Strömberg and Banwart ((10) their Table 4). ^e Tracer release rate estimated as $\sum Q_i C_i / M$ where Q_i is water flow and C_i is tracer concentration in drainage ditch i of the two drainage ditches at the Aitik site reported by Strömberg and Banwart ((8) their Table 1) and M is the total waste rock mass (Table 1). ^f Corrected for chalcopyrite dissolution.

different observation scales listed in Table 1. Table 2 lists both the obtained mass normalized rate, $R^{B/C/F}$ (mol kg⁻¹ s⁻¹), and the associated, surface area normalized rate coefficient, $k^{B/C/F}$ (mol m⁻² s⁻¹), with the label B/C/F referring to the batch/column/field observation scale. Table 2 reveals a significant scale-dependence, with weathering rates that are 1–3 orders-of-magnitude lower in the field than in the batch experiments and with the rates for the large column experiments in between. The scale-dependence is different for the different minerals (chalcopyrite > biotite ≈ pyrite > plagioclase). Overall, however, the scale-dependence is consistent with previous comparative observations of mineral weathering in the laboratory and the field (1–6), supporting the use of the Aitik site as a quite general model system for studying scale-dependent mineral weathering rates.

Method

Table 1 shows that there are relatively small but potentially important differences in temperature, pH, and mineral content between the observation scales. Hydrologically, the three scales also represent a range of different conditions: full water saturation and no flow in the batch reactors (9), unsaturated (water content of about 10 vol %) and relatively homogeneous flow in the column experiments (11), and unsaturated flow in the field (about 10 vol % total water content) with about 35% of the total water content being relatively immobile (11). Furthermore, the particle size distribution differs between the three observation scales (Figure 1 in the Supporting Information), and particle size has in the batch experiments (9) been found to significantly influence weathering rates for some minerals in the Aitik waste rock ((9) Table 2 in the Supporting Information).

We quantified scaling factors associated with these identified differences in the physicochemical characteristics: temperature, pH, mineral content, hydrological flow paths, and particle size distribution. We propose to use the scaling factors for extrapolating batch rate coefficients, k^b , and independently (i.e., without any model calibration to observed results) predicting column/field-scale weathering rates, $R^{C/F}$, as

$$\frac{R^{C/F}}{a_{sm}^{C/F}} = \alpha^{C/F} \beta_T^{C/F} \beta_{pH}^{C/F} \beta_{PS}^{C/F} k^b \quad (1)$$

The factor $\alpha^{C/F}$ is hydrological and accounts for the potential existence of preferential flow paths and immobile water (11, 13–16). For the Aitik case, it has been experimentally quantified (11) as the ratio between mobile and total water content in hydrological tests using unreactive tracers ((11) $\alpha^F = 0.65$ and $\alpha^C = 1$). The different β factors represent a correction of the batch rate coefficient, k^b , for temperature, pH, and particle size. The correction for temperature is quantified as $\beta_T^{C/F} = \exp[-E_a/R_g(1/T^{C/F} - 1/T^b)]$ based on the Arrhenius' equation, with E_a being the activation energy, R_g the universal gas constant, and T the absolute temperature at each scale. The pH effect is accounted for as $\beta_{pH}^{C/F} = 10^{n(pH^b - pH^{C/F})}$ with n being the reaction order with respect to protons. For the individual minerals, we use activation energies and reaction orders from the literature (Table 3 in the Supporting Information). The correction for the particle size effect is quantified as $\beta_{PS}^{C/F} = \sum_i^{C/F} x_i k_i / k^b$ with x_i being the particle size fraction that is associated with the rate coefficient k_i . The product $x_i k_i$ is summed over the entire particle size distribution at the considered scale (Figure 1 in the Supporting Information). The rate coefficients, k_i , were obtained from the batch experiments, in which individual size fractions were studied separately ((10) Table 2 in the Supporting Information). Moreover, the quantification of the specific mineral surface area, $a_{sm}^{C/F} = \gamma_m^{C/F} a_s$, where γ_m is the mineral content and a_s is the total specific surface area, implies an additional scaling factor, accounting for differences in mineral distribution between the observation scales. For the Aitik case, γ_m has been determined by point counting using light microscopy ((8) Table 1 in the Supporting Information), and a_s has been determined using the BET-method and is constant on all scales ((9) $a_s = 1000$ m² kg⁻¹), yielding the scaling factor $a_{sm}^{C/F} / a_{sm}^B = \gamma_m^{C/F} / \gamma_m^B$.

Results and Discussion

Figure 1 illustrates the comparison between predicted weathering rates, according to the proposed eq 1, and

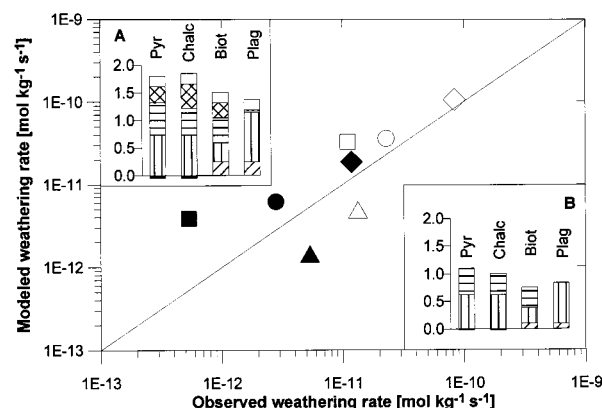


FIGURE 1. Modeled field and column scale weathering rates plotted against observed weathering rates (R^{CF} in Table 2), i.e., against the rates that were estimated directly from observed tracer release rates. Modeled field and column rates were predicted according to the proposed eq 1, which upscales the batch rate coefficients, k^B , listed in Table 2. Open and filled symbols denote the column and the field scale, respectively (\diamond pyrite, \square chalcopyrite, \circ biotite, \triangle plagioclase). The solid line represents the ideal case, "perfect prediction", where modeled rates equal observed rates. The inserts show the logarithmic values of the scaling factors for the field (insert A) and the columns (insert B) according to the following: hatched pattern, $-\log \beta_{pH}^{CF}$; vertical lines, $-\log \beta_T^{CF}$; horizontal lines, $-\log \beta_{PS}^{CF}$; cross-hatched pattern, $-\log \gamma_m^{CF} \gamma_m^{CF}$; and \square , $-\log a^{CF}$. \blacksquare denotes overlap of the $-\log \beta_{pH}^{CF}$ and the $-\log \beta_T^{CF}$ due to negative $-\log \beta_{pH}^{CF}$ values for the sulfides.

observations (Table 2), along with the individual contributions of the different scaling factors for the Aitik data. The results show that the quantified physicochemical effects can to a large degree explain the observed scale-dependence in mineral weathering rates for the Aitik case study. Figure 1 also shows that the relative importance of the different correction factors varies over the scales and between the individual minerals. The remaining discrepancy between model results and observations is generally larger for the field than for the columns. In the column experiments, conditions were much more homogeneous and controlled than in the field, where, for instance, copper immobilization in local pore water zones with higher pH than the drainage water may be one reason for the relatively large discrepancy for chalcopyrite. Such immobilization processes are not considered in our model, which is focused on the effects of directly observable, bulk-averaged physicochemical characteristics at the different experimental scales.

Our proposed model expresses a general methodology, applicable for different minerals, to extrapolate laboratory rate data to other scales and conditions through the use of mutually independent correction factors. For the Aitik site, the model accounts for differences in the average temperature, pH, mineral content, flow paths, and particle size distributions between the scales. For other sites, additional important physicochemical characteristics may also differ between the different scales and must then be represented by additional scaling factors. Processes that affect the tracer fluxes, besides the weathering of primary minerals, may also prevail under other site-specific conditions and must then be conceptualized and modeled.

Our actual quantifications of the correction factors are based on differences in readily available, bulk-averaged characteristics at the different scales, thus representing a consistent level of model complexity for each and all of the considered effects. For the Aitik case, the quantification of the particle size effect was based on experimental studies (9). There is no underlying process description for this factor,

which thus is empirical and site-specific. In contrast, the quantifications of the effects of temperature, pH, and preferential flow were process-based (mechanistic) through the use of the Arrhenius' equation, rate laws for mineral weathering, and the mobile to immobile water content, respectively. For the site-specific quantification of the temperature and pH factors, we assumed, based on previously published results (8–10), that the weathering processes are rate limited by abiotic surface reactions.

Application of the proposed model to other sites and conditions, where microbially mediated weathering may predominate, would still require correction for all factors included in our model (eq 1). However, the actual quantifications of the temperature and pH factors must then be based on parameters and mechanistic or empirical relations that are valid for the specific biotic reactions at the site. The quantification of the effect of preferential flow is independent of the nature of the weathering process and would be the same for biotic and abiotic weathering processes. Moreover, the quantification of the particle size effect is empirical and site-specific. Experimental determination of this effect would thus apply also for biotic weathering processes as well as implicitly account for potential diffusional resistance to weathering in large particles.

The fact that the scale-dependence exhibited by the Aitik data is consistent with other laboratory and watershed studies (1–6) suggests that at least some of the effects identified here are of general applicability and importance when extrapolating weathering rates from the laboratory to the field. The proposed model of scale-dependence (eq 1) due to these effects was in the Aitik case successful for a range of different minerals (sulfides and silicates) and observation scales (extrapolating from batch to both large columns and the field), and it was independent of any model calibration to observed results. Based on this success, we think that this scale-dependence model is worthy of further testing, across a wider range of weathering conditions at the field scale.

Acknowledgments

This research was funded by the Swedish Foundation for Strategic Environmental Research (MISTRA) through the research program "Mitigation of the environmental impact from mining waste" (MiMi).

Supporting Information Available

Tables 1 (mineralogy of the Aitik waste rock heaps), 2 (rate coefficients for different size fractions), and 3 (literature values on activation energy and reaction order) and Figure 1 (cumulative mass fractions for column experiments and the field site). This material is available free of charge via the Internet at <http://pubs.acs.org>.

Literature Cited

- (1) Schnoor, J. In *Aquatic Chemical Kinetics*; Stumm W., Ed.; John Wiley and Sons: New York, 1990.
- (2) White, A. F.; Peterson, M. L. In *Chemical Modeling of Aqueous Systems II*; Melchior, D. L., Bassett, R. L., Eds.; ACS Symposium Series 416; American Chemical Society: Washington, DC, 1990.
- (3) Swoboda-Colberg, N. G.; Drever, J. I. *Chem. Geol.* **1993**, *105*, 51.
- (4) Velbel, M. A. *Chem. Geol.* **1993**, *105*, 89.
- (5) Drever, J. I.; Murphy, K. M.; Clow, D. W. *Min. Magn.* **1994**, *58A*, 239.
- (6) Drever, J. I.; Clow, D. W. In *Reviews in Mineralogy Vol. 31: Chemical Weathering Rates of Silicate Minerals*; White, A. F., Brantley, S. L., Eds.; Mineralogical Society of America: Washington, DC, 1995.
- (7) White, A. F.; Brantley, S. L. *Reviews in Mineralog.* **Vol. 31: Chemical Weathering Rates of Silicate Minerals**; Mineralogical Society of America: Washington, DC, 1995.
- (8) Strömberg, B.; Banwart, S. *Appl. Geochem.* **1994**, *9*, 583.
- (9) Strömberg, B.; Banwart, S. *Appl. Geochem.* **1999**, *14*, 1.
- (10) Strömberg, B.; Banwart, S. *J. Cont. Hydrol.* **1999**, *39*, 59.

- (11) Eriksson, N.; Gupta, A.; Destouni, G. *J. Hydrol.* **1997**, *194*, 143.
- (12) Eriksson, N.; Destouni, G. *Water Resour. Res.* **1997**, *33*, 47.
- (13) Van der Zee, S. E. A. T. M.; Boesten, J. J. T. I. *Water Resour. Res.* **1991**, *27*, 3051.
- (14) Gaber, H. M.; Inskeep, W. P.; Comfort, S. D.; Wraith, J. M. *Soil Sci. Soc. Am. J.* **1995**, *59*, 60.
- (15) Destouni, G.; Sassner, M.; Jensen, K. H. *Water Resour. Res.* **1994**, *30*, 747. (Correction, *Water Resour. Res.* **1995**, *31*, 1161).
- (16) Gupta, A.; Destouni, G.; Bergen Jensen, M. *J. Cont. Hydr.* **1999**, *35*, 389.

Received for review June 17, 1999. Revised manuscript received December 15, 1999. Accepted January 28, 2000.

ES990682U